STRATEGIES FOR THE USE OF LANTHANIDE NMR SHIFT PROBES IN THE DETERMINATION OF PROTEIN STRUCTURE IN SOLUTION

Application to the EF Calcium Binding Site of Carp Parvalbumin

Lana Lee and Brian D. Sykes, *MRC Group on Protein Structure and Function, and Department of Biochemistry, University of Alberta, Edmonton, Alberta, Canada T6G 2H7*

ABSTRACT   The homologous sequences observed for many calcium binding proteins such as parvalbumin, troponin C, the myosin light chains, and calmodulin has lead to the hypothesis that these proteins have homologous structures at the level of their calcium binding sites. This paper discusses the development of a nuclear magnetic resonance (NMR) technique which will enable us to test this structural hypothesis in solution.   The technique involves the substitution of a paramagnetic lanthanide ion for the calcium ion which results in lanthanide induced shifts and broadening in the ^{1}H NMR spectrum of the protein.   These shifts are sensitive monitors of the precise geometrical orientation of each proton nucleus relative to the metal. The values of several parameters in the equation relating the NMR shifts to the structure are however unknown *a priori*.   We have attempted to determine these parameters, the orientation and principal elements of the magnetic susceptibility tensor of the protein bound metal, by studying the lanthanide induced shifts for the protein parvalbumin whose structure has been determined by x-ray crystallographic techniques.   The interaction of the lanthanide ytterbium with parvalbumin results in high resolution NMR spectra exhibiting a series of resonances with shifts spread over the range 32 to -19 ppm.   The orientation and principal elements of the ytterbium magnetic susceptibility tensor have been determined using three assigned NMR resonances, the His-26 C2 and C4 protons and the amino terminal acetyl protons, and seven methyl groups; all with known geometry relative to the EF calcium binding site. The elucidation of these parameters has allowed us to compare the observed spectrum of the nuclei surrounding the EF calcium binding site of parvalbumin with that calculated from the x-ray structure. A significant number of the calculated shifts are larger than any of the observed shifts.   We feel that a refinement of the x-ray based proton coordinates will be possible utilizing the geometric information contained in the lanthanide shifted NMR spectrum.

INTRODUCTION

Calcium binding proteins play an important role in the regulation of many biochemical processes (1, 2).   Among the most studied of these proteins are the skeletal and cardiac troponins (3), and myosin light chains (4), which are involved in the regulation of muscle contraction; and calmodulin (5) from brain which is involved in the regulation of cyclic nucleotide phosphodiesterase activity. The elucidation of the x-ray structure of the calcium binding protein parvalbumin from carp revealed that its two calcium binding sites are each completely formed from a contiguous polypeptide sequence folded into the homologous "CD and EF hands" (6). Each calcium binding site contains in turn a helix, a loop around the metal

ion, and a second helix. The loop around the metal ion contains regularly spaced liganding carboxyl or carbonyl ligands. Homologous sequences to parvalbumin (1, 7–9) can be found in many other calcium binding proteins such as those listed above. The number of times in a given protein the sequence repeats, and the substitutions therein, can be correlated with the number of metals bound to the protein and their binding strengths, respectively. These findings have lead to the proposal that homologous structures, at least at the level of the calcium binding sites, exist for all these proteins.

In this paper we shall describe the development of a NMR technique, the final goal of which is the ability to compare in detail protein structures in solution. This technique will then enable us to test the hypothesis that all of these calcium binding proteins have homologous structures. The technique is based upon the substitution of paramagnetic lanthanide ions for the calcium ions and the subsequent analysis in structural terms of the shifts and broadenings induced in the NMR spectrum (^{1}H NMR in this specific example). Our approach is to study carp parvalbumin (pI=4.25) initially, and to use the known x-ray structure of this protein to determine the unknown parameters of the NMR experiment which are required before the shifts and broadenings can be interpreted in terms of the structure of the protein. With these parameters, and the knowledge of the amino acid substitutions for different proteins, we will then be able to compare the calculated and observed NMR spectra of a new protein as a probe of its structure. This approach requires first and foremost that the lanthanides replace the calcium with no structural change. This is clearly supported for parvalbumin by several lines of evidence including the x-ray studies of terbium substituted parvalbumin (10) and the laser fluorescence (11) studies of terbium and europium substituted parvalbumins.

Lanthanide induced shifts have been used previously to probe structural details of proteins including lysozyme (12, 13) and the bovine pancreatic trypsin inhibitor (14–16). Neither of these proteins have calcium specific metal binding sites; the metal binding ligands being two carboxyls in the active site of lysozyme and nitrotyrosyl side chains of the trypsin inhibitor. The biggest difference in our application is that the metal binding is tight and specific. This has a dramatic influence on the form of the NMR experiment. In the previous examples, the weak metal ion binding has lead to NMR spectra (of mixtures of metal and protein) which are in the NMR fast exchange limit. This has the advantage that the influence of the paramagnetic metal ion can be progressively followed for assigned resonances, but has the disadvantages that non-specific binding can influence the results and therefore chemical shifts and relaxation times characterizing the spectrum of the protein metal complex have to be determined by extrapolation to infinite metal concentration. When the metal binding is tight and specific, the spectrum of the metal protein complex can be readily observed and the shifts and relaxation times of the protein metal complex accurately determined. The main disadvantage is the difficulty in assigning the observed shifted peaks. A parallel set of examples that have been studied are the binding of Co^{++} to lysozyme (17, 18) which was in the NMR fast exchange limit, and the binding of Co^{++} to concanavalin A (19) which was in the NMR slow exchange limit.

As a consequence of the above, previously obtained lanthanide induced NMR shifts and relaxation times have not been determined accurately enough to prove more than a general consistency between the x-ray and the solution structure (12–16). Our NMR measurements provide structural detail at a potential resolution much higher than that presently obtainable from x-ray diffraction because of the high order dependence on distance involved in the NMR experiment. The problem at present is how to unravel this data and that will be the focus of

this manuscript. We shall attempt to describe the approach we have taken to the acquisition of the NMR data for parvalbumin (most of which will be presented in detail elsewhere), to the interpretation of this data, and to the implications of the result with respect to the x-ray structure. A significant number of the calculated shifts are larger than any of the observed shifts. We feel that a refinement of the x-ray based proton coordinates will be possible utilizing the geometric information contained in the lanthanide shifted ^{1}H NMR spectrum.

STRATEGY OF THE APPROACH AND APPROPRIATE NMR THEORY

All of the discussion below, of the NMR theory and its application, will be described in terms of our particular application to the protein parvalbumin.

Theory of the Lanthanide Induced Shifts

When a paramagnetic lanthanide ion (excluding the isotropic Gd^{+3}) is substituted for one or both of the calcium ions of parvalbumin, a series of shifted resonances appear in the ^{1}H NMR spectrum far outside of the envelope of the spectrum of the calcium form of the protein. The shifted peaks in these spectra, shown in Fig. 1 for Yb^{+3}, are in the NMR slow exchange limit and therefore represent the spectrum of the protein-paramagnetic metal ion complex. The shifts result from the influence of the 4f electrons of the lanthanide metal on nearby ^{1}H nuclei and can be divided into two contributions. The first is a through space dipolar ("pseudo-contact") interaction. The magnitude of the pseudo-contact shift is a function of the metal ion involved and of the geometry of the proton relative to the metal ion. The shift of the nucleus
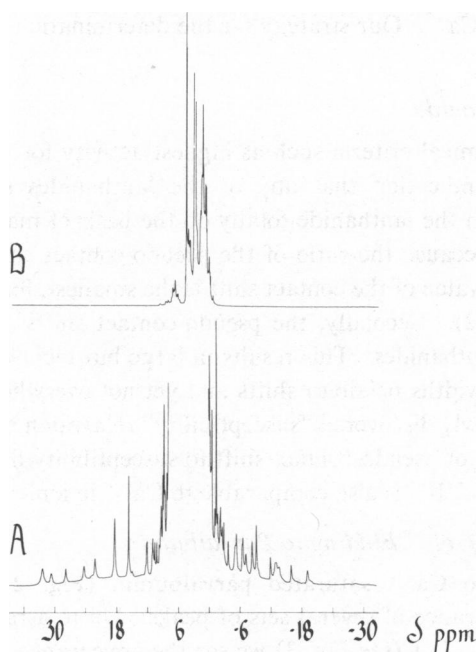

Figure 1   The 270-MHz ^{1}H-NMR spectrum of: (a) 1.0 mM parvalbumin in 15 mM Pipes, 0.15 M KCl, 0.5 mM DSS in D_2O, pH 6.65 at a total (Yb^{+3}_o/protein$_o$) ratio of 0.96. Temperature = 303°K. (b) 1.1 mM calcium saturated parvalbumin in 15 mM Pipes, 0.15 M KCl, 0.5 mM DSS in D_2O, pH 6.65. All chemical shifts mentioned in this manuscript are measured relative to the principal resonance of DDS-sodium 2,2-dimethyl-2-silapentane-5-sulfonate.

from its diamagnetic position written in the principal axis system of the magnetic susceptibility tensor of the metal ion is (20):

$$\delta_P = A_1 \left\langle \frac{3 \cos^2 \theta - 1}{r^3} \right\rangle + A_2 \left\langle \frac{\sin^2 \theta \cos 2\phi}{r^3} \right\rangle \equiv A_1 G_1 + A_2 G_2 \qquad (1)$$

where A_1 and A_2 are parameters of the metal ion related to the principal elements of the magnetic susceptibility tensor, r, θ, and ϕ are the spherical coordinates of the nucleus in the principal axis system, and the $<>$ brackets indicate that the appropriate time averaged geometry of the nucleus must be used in the calculation (21). With order of magnitude values of $A_1 \simeq A_2 \simeq 1,000$ ppm Å^{+3} from other experiments (15), we see that nuclei in the range of $\simeq$ 4 Å from the metal can have shifts as large as $\simeq 50$ ppm whereas nuclei $\simeq 10$ Å from the metal will have shifts only as large as $\simeq 3$ ppm. The second contribution to the shifts is a through bond contact interaction which is important for directly bonded nuclei such as ^{13}C and ^{17}O and generally less important for the lanthanides when compared with the transition metals. We are looking at ^1H nuclei several bonds removed and attempt further to minimize this contribution by choice of metal (see below) since the geometric dependence of this contribution to the shift is not known *a priori*.

For the interpretation of our experiments we are interested in calculating the NMR shifts for the protons of parvalbumin assuming in the first iteration the known geometry from the x-ray structure. For the pseudo-contact shift this requires knowledge of five unknowns: the three Euler angles (α, β, γ) characterizing the orientation in the protein of the principal axis system of the magnetic susceptibility tensor of the metal; and the two parameters $A_1 = (X_{xx}-\overline{X})$ and $A_2 = (X_{xx}-X_{yy})$ where X_{xx}, X_{yy}, X_{zz}, and $\overline{X}$ are the principal elements and trace respectively of the magnetic susceptibility tensor. We will assume that the Yb^{+3} is located at the same position as the Ca^{+2}. Our strategy for the determination of these five unknowns is discussed below.

Choice of Lanthanide

In the absence of biochemical criteria such as highest activity for the choice of a particular lanthanide (or of any indication that any of the lanthanides significantly perturb the structure) we have chosen the lanthanide totally on the basis of magnetic criteria. We have chosen Yb^{+3} primarily because the ratio of the pseudo-contact shift to the contact shift is largest, and the absolute value of the contact shift is the smallest, for Yb^{+3} when compared to the other lanthanides (22). Secondly, the pseudo-contact shifts are relatively large when compared to the other lanthanides. This results in large but technologically manageable (in terms of spectral sweep widths possible) shifts and yet not overwhelming broadening of the shifted peaks from the newly discovered "susceptibility" relaxation mechanism (23, 24). This resolution criterion (ratio of pseudo-contact shift to susceptibility line broadening) has been discussed elsewhere (25). Yb^{+3} is also comparable to Ca^{++} in ionic radius (26).

Stoichiometry of Yb^{+3} Binding to Parvalbumin

When Yb^{+3} is added to Ca^{++} saturated parvalbumin (Fig. 2) we see the sequential appearance and disappearance of several sets of peaks. Up to a ratio of total Yb^{+3} to total parvalbumin (Yb_o/P_o) of ~1/1 (see Fig. 3) we see the appearance of one set of peaks which correspond to nuclei in the region of the first calcium replaced. As the second calcium is replaced at higher Yb_o/P_o ratios, some resonances such as that at 15.17 ppm[1] and indicated by

---

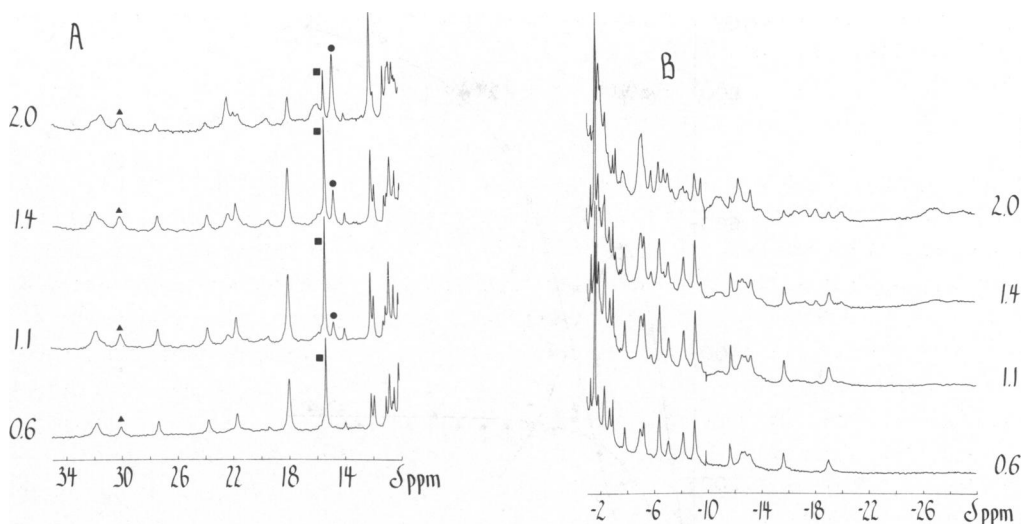[1]All chemical shifts when quoted precisely refer to spectra taken at 30°C.

Figure 2 The 270-MHz ^{1}H-NMR spectrum of 0.84 mM carp parvalbumin in 15 mM Pipes, 0.15 M KCl, 10 mM DTT, 0.5 mM DSS in D_2O, pH 6.63, at total $(Yb^{+3}_o/protein_o)$ ratios of 0.6, 1.1, 1.4, and 2.0. Ambient temperature – 303°K. (a) Downfield region of spectrum; ■, ●, and ▲ indicate peaks plotted in Fig. 3. (b) Upfield region of spectrum; spike near -10 ppm is an instrumental artifact.

a ■ in Fig. 3 disappear and are replaced by a new set of resonances. The resonances which appear and then disappear must be near to and influenced by both metal sites, while the resonances which appear and then remain constant (typified by the peak at 29.80 ppm and indicated by ▲ in Fig. 3) must be near the first calcium replaced but removed from the second. Those that appear only after the first site is filled (such as the peak at 14.55 ppm and indicated by a ● in Fig. 3) must be either influenced by both metals or only the second metal. This experiment allows us to determine the relative affinities of the two sites, which will not be discussed here. The areas of these peaks, which are also obtained as a part of the fitting procedure used to determine the calculated curves in Fig. 3, are however important and allow us to discriminate single protons from methyl groups. Fig. 3 is again illustrative where the calculated areas of peaks at 14.55 and 15.17 ppm are 983 ± 57 and 804 ± 24, respectively, whereas the area of the peak at 29.80 ppm is 304 ± 13. In this manner, in conjunction with the temperature experiments discussed below, we have been able to identify six shifted methyl resonances nearby the first calcium site which is replaced. These methyls have been used extensively in the fitting procedure since they are distinctive and there are not that many methyl groups near the calcium binding sites (only seven within 10 Å of the EF calcium site, for example).

All of these spectra have been taken with NMR recycle times long enough, relative to the spin lattice relaxation rates, that the areas represent true relative intensities. One further point is that not all of these resonances are necessarily carbon bound. Experiments with parvalbumin where all of the NH protons have been preexchanged for ND have indicated that the peak of 12.00 ppm, for example, is an NH peak.

We are thus able to see the sequential filling of the two metal binding sites, to characterize the proximity of the shifted peaks to the two sites and to measure their relative areas. This experiment does not, however, tell us which metal site of parvalbumin is filled first. For this we must draw on other evidence such as the x-ray analysis (10) and optical experiments (27) on the partially terbium substituted protein. We shall assume henceforth that these
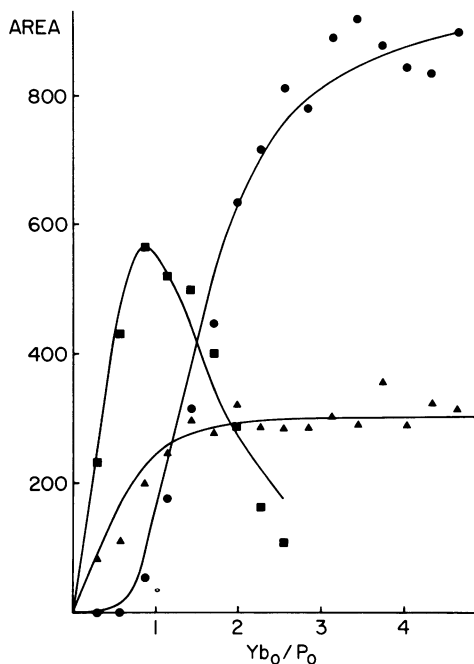
Figure 3   The areas of three representative peaks as a function of $(Yb^{+3}_0/protein_0)$ ratio, where resonances represented by ▲, ■, and ● have chemical shifts of 29.80, 15.17, and 14.55 ppm, respectively (see Fig. 2 *a*).

experiments are correct, and that it is the EF calcium that is replaced first.   All further discussion will concentrate on the shifted peaks observed in spectra up to a Yb_0/P_0 ratio of 1/1 where only the EF calcium has been replaced.

Temperature Dependence of the Shifted Resonances

While we can easily and accurately observe these shifted resonances, we do not know their origin in the diamagnetic spectrum (δ_D).   We measure the observed shift (δ_{OBS}) and do not know the paramagnetic contribution $(\delta_P = \delta_{OBS}-\delta_D)$.

We have been able to deduce experimentally the origin of each peak in the diamagnetic spectrum by following the temperature dependence of the shifted resonances.   As the temperature is raised, the thermal population of higher electronic states leads to a more isotropic electronic distribution and smaller shifts (28). If the structure of the protein metal complex is stable over a reasonable temperature range, the shifts can be measured as a function of temperature and the observed shifts formally extrapolated to infinite temperature which corresponds to zero paramagnetic shift.   Fig. 4 shows some of the spectra in the temperature range studied of 4°C to 59°C.   This temperature dependence is very useful in sorting out overlapping peaks and confirming the contributions to the area of overlapping peaks as can be seen by the resonances marked by ▲, ■, and ●.

To analyze the temperature dependence we first assumed that the diamagnetic shift is temperature independent, that the geometric factors in Eq. 1 are temperature independent and that the dependencies of A_1 and A_2 on temperature are equal.   The temperature dependence of the shift is then given in general by (20, 28):

$$\delta_{OBS} - \delta_D = \delta_P = \frac{A}{T^2} + \frac{B}{T^3} + \frac{C}{T^4} + \cdots,\qquad(2)$$
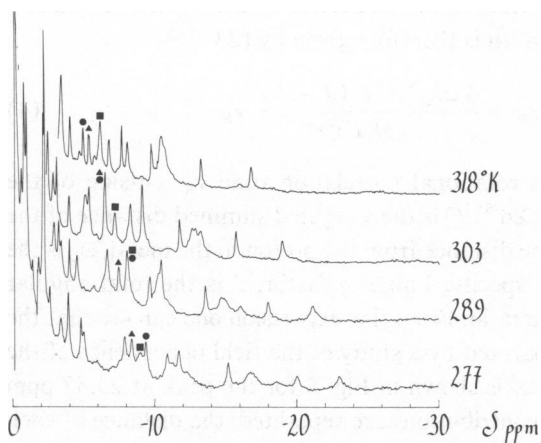
Figure 4

Figure 5

Figure 4   The upfield region of the 270-MHz ^{1}H-NMR spectra of 0.8 mM parvalbumin in 15 mM Pipes, 0.15 M KCl, 10 mM DTT, 0.5 mM DSS in D$_2$O, pH 6.65, at a total (Yb^{+3}$_o$/protein$_o$) ratio of 0.8 as a function of temperature, (277°, 289°, 303°, and 318°K).

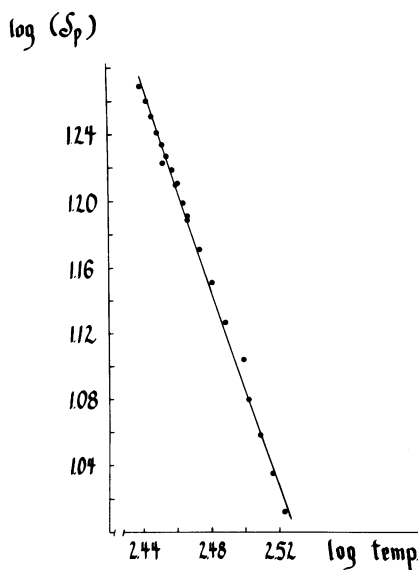**Figure 5**   The temperature dependence of the chemical shift of the resonance with δ^{OBS} – 15.17 (at 303°K) indicated by a plot of log (δ_P) vs log temperature.

where A, B, and C are constants. The contributions of the various terms with increasing powers of $1/T$ to the temperature dependence was estimated by plotting the shift (δ_p) of the methyl resonance at 15.17 ppm vs. log $(1/T)$. Choosing reasonable values for δ_D of a methyl resonance in the range of 0 to 2 ppm lead to values of the slope n in the range 2.8–3.2.· Fig. 5 shows a plot for this methyl resonance of log(δ_P) versus log T for the choice $\delta_D = 1$ ppm. The absence of breaks in this plot is taken as an indication of no structural conformational changes over this temperature range.   The diamagnetic shifts for all of the other protons were determined relative to the choice of $\delta_D = 1$ ppm for the methyl group at 15.17 ppm by assuming that all of the resonances extrapolate similarly towards $1/T^n = 0$, which implies:

$$\delta^i_{OBS} - \delta^i_D = K(\delta^j_{OBS} - \delta^j_D), \tag{3}$$

where K is a constant, and i, and j are two shifted resonances. The diamagnetic shift of peak i is then obtained by plotting shifts pairwise vs. the methyl group at 15.17 ppm. No value of n is assumed in these plots. The diamagnetic shifts so obtained were sensitive to various extents to the choice of $\delta_D = 1$ for the methyl group at 15.17 ppm. For example, the calculated value of δ_D for the resonance with $\delta_{OBS} = 29.80$ ppm was fairly sensitive and varied between 2.18 and 4.13 ppm as δ_D for the methyl resonance at 15.17 ppm was varied between 1 and 2 ppm. This represents, however, only a variation of 7% in the value of δ_P for this resonance. This is the least solid of our experimental data, but the variations involved do not affect in any way the conclusions we draw in this paper.

Analysis of the Linewidths of Shifted Resonances

The linewidths of the shifted nuclei are determined by three contributions: dipole-dipole interactions with neighboring nuclei, dipolar interaction of the Solomon-Bloembergen type

with the 4f electrons of the lanthanide (29), and dipolar interaction with the "Curie spin" of the metal (23, 24). Scalar relaxation through contact interactions are neglected as stated above. As discussed elsewhere (25), the Curie spin or susceptibility contribution far outweighs the Solomon-Bloembergen contribution to the linewidths of the shifted resonances in the Yb^{+3} parvalbumin complex. The linewidth is therefore given by (23–25):

$$\pi\Delta\nu = \frac{9}{20}\gamma^4\hbar^2\sum\left(\frac{1}{d^6}\right)\tau_R + \frac{4}{5}\frac{\omega_0^2 g_L^4 \beta^4 J^2 (J+1)^2}{(3kT)^2 r^6}\tau_R \tag{4}$$

for an isotropically tumbling molecule with rotational correlation time τ_R, outside of the extreme narrowing limit $(\omega_0\tau_R)^2 > 1$, where $(\Sigma d^{-6})^{1/6}$ is the weighted summed distance of the observed proton to neighboring protons, r is the distance from the proton to the metal, ω_0 is the proton resonance frequency, g_L is the metal specific Landé g factor, J is the total angular momentum, and γ is the proton gyromagnetic ratio. From this expression one can see that the two contributions to the linewidth can be separated by a study of the field dependence of the linewidth. A typical plot of linewidth verus ω_0^2 is shown in Fig. 6 for the peak at 23.57 ppm and the CH_3 group at 15.17 ppm. Once the contributions are separated, the distance of each of the shifted nuclei from the metal ion can be ascertained (see Fig. 7) with the value of $\tau_R = 12 \times 10^{-9}$ secs taken from separate experimental sources (30).

Determination of the NMR Unknowns which Relate Observed Shifts to Structure

At this stage several attempts were made to solve the relationship between the observed shifts of the nuclei near the metal ion and their geometry with respect to the metal ion. This involves, as we have discussed above, the determination of the orientation (specified by three
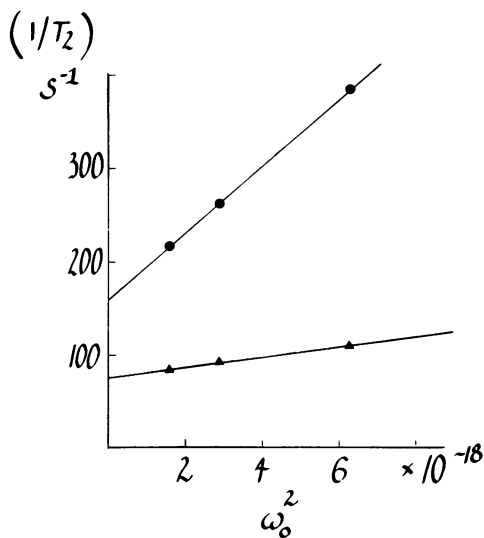

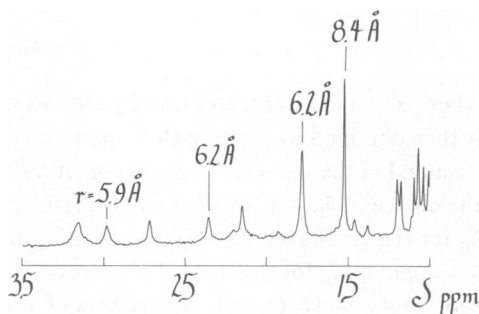Figure 6   Figure 7

Figure 6   The linewidth of resonances with chemical shifts 23.57 ppm (●) and 15.17 ppm (▲) as a function of field. Linewidths were measured at 200, 270, and 400 MHz. The sample was 0.67 mM parvalbumin in the standard buffer, pH 6.68, at a (Yb^{+3}_o/protein$_o$) ratio of 1.0.

Figure 7   Representative metal to proton distances calculated from the field dependent contribution to the linewidth.

angles α, β, and γ) of the principal axis system of the magnetic susceptibility tensor, centered on the metal, and of the magnitude of two scaling parameters (A_1 and A_2) related to the principal elements of this tensor. The data we know for each shifted resonance include its paramagnetic shift, its area, its relative proximity to the EF and CD sites, its diamagnetic shift, its diamagnetic linewidth, its distance from the metal ion and whether it is C or N bound. One useful subset was the identification by area of six shifted methyl resonances, since there are a total of only seven methyls within 10 Å of the EF metal binding site. Two of tsfe methyls are shifted more downfield than 10 ppm, and appear at 17.79 ppm ($\delta_P = 17.69$ ppm) and 15.17 ppm ($\delta_P = 14.17$ ppm) in Fig. 2. The other four observed are shifted upfield, the most upfield shifted appearing at -1.59 ppm ($\delta_P = -1.90$ ppm). Two of these upfield shifted methyls are seen overlapping at $\delta = -1.6$ ppm in Fig. 2 B. We also need to know the coordinates of the protons surrounding the metal in order to calculate spectra based upon the known x-ray structure. The last Diamond refined X-ray structure of parvalbumin (31) was chosen as the most appropriate starting point. Proton coordinates were generated from this structure assuming standard bond lengths and geometries. In the case of methyl groups, the "methyl proton centroid" model (32) was used to determine the average methyl proton positions. We then proceeded to calculate spectra from the x-ray based proton coordinates for various choices of A_1, A_2, α, β, and γ and to compare the calculated and observed values of δ^i_P. Several criteria were used in an attempt to assess the goodness of fit between the calculated and observed spectra to evaluate choices of the unknowns A_1, A_2, α, β, and γ. These criteria were based mainly upon the observed shifted methyl resonances. After many attempts, no unambiguous fit was calculated and a second approach to the fitting procedure was initiated.

In the diamagnetic spectrum of carp parvalbumin (which contains 10 Phe, 1 His, 0 Tyr, 0 Trp), three resonances could be assigned to specific nuclei. These were the C_2 and C_4 protons of His 26 and the CH_3 group on the acetylated amino terminus, each of which could be detected because of its distinctive chemical shift, area, and relatively narrow linewidth. The pH titration behavior of the His 26 C_2 and C_4 proton resonances confirmed their assignment. Although these nuclei are all relatively far removed from the metal (13–20 Å), their resonances are shifted, and the resulting spectra are in the slow exchange limit. Since the shifts and linebroadening were small, the shifted peaks were also easily assigned by the same methods. The shifts of these three assigned resonances were then used to determine the NMR unknowns in conjunction with the methyl group shifts. In this regard the fact that these assigned nuclei are relatively far removed from the metal turned out to be an advantage because their calculated geometric factors, G_1 and G_2 from Eq. 1, were not sensitive to inaccuracies in the x-ray structure. The histidine and the N-acetyl nuclei are also situated at diverse angular orientations which is advantageous for the fitting procedure. The search for the best fit solution to the NMR unknowns was made in the following manner. For a given choice of α, β, and γ, the geometric factors G_1 and G_2 were calculated for the His C_2, His C_4 and N-acetyl CH_3 protons. The parameters A_1 and A_2 for this particular choice of axis system were then taken as those giving the best least squares fit of the calculated shifts to the observed shifts for these nuclei. If the resultant calculated shifts for the assigned resonances were in good agreement with the observed shifts, the shifts of the CH_3 groups near the EF site were then calculated from their geometry in this axis system and the best fit A_1 and A_2. The choice of axis system was then rejected if it did not meet the criterion of having only two methyl groups shifted more downfield than 10 ppm, and no methyl resonance shifted more upfield than -5 ppm. If the solution passed the above criterion, the goodness of the solution was tested by calculating a chi value comparing the two calculated most downfield methyl

TABLE I
CHEMICAL SHIFT DATA OF THE ASSIGNED HISTIDINE AND
N-ACETYL RESONANCES OF PARVALBUMIN

Nucleus	Observed*			Calculated	
	δ_{OBS}	δ_D	δ_P	δ_P	r(Å)
His 26 C$_2$	8.038	7.553	0.485	0.488	13.6
His 26 C$_4$	7.159	6.816	0.343	0.337	15.1
N-Acetyl	2.083	2.050	0.033	0.042	20.1

*Chemical shifts are measured in ppm.

shifts with the observed values of δ_P = 17.69 and 14.17 ppm, and the calculated most upfield methyl shift with the observed δ_P = -1.9 ppm. One best fit solution was identified on the basis of the best fit of the calculated shifts to the His C$_2$, His C$_4$, and N-acetyl shifts and the three shifted methyls discussed above. In fact, 24 solutions were found corresponding to the various possible permutations of the labeling of the principal axis system (13), the final solution selected by adopting the convention that $|A_1|$ be maximal, and that $0 < |A_2/A_1| < 1$.

In practice, our best fit solution was calculated in terms of the direction cosines L1, L2, and L3 (L1^2 + L2^2 + L3^2 = 1) and rotation angle α involved in the transformation of the coordinates of the protons from the x-ray structure axis system to a new axis system. The values for the best fit solution are L1 = -0.60, L2 = -0.77, L3 = -0.217, and α = 4.11 radians, with the values of A_1 and A_2 equal to -5,450 ppm Å^3 and -3,360 ppm Å^3, respectively.

RESULTS

The measured chemical shifts of the His 26 C$_2$, His 26 C$_4$, and N-acetyl protons of parvalbumin are listed in Table I, both in the presence of Ca^{+2} and Yb^{+3}. The calculated shifts of these protons come from the best fit solution obtained in the manner described above. There is excellent agreement between the calculated and observed results here, indicated by a standard deviation of ±0.008 ppm. The paramagnetic shifts for the observed methyl groups and the distances obtained from their linewidths are listed in Table II. Also listed are the best fit calculated shifts, and the distances based upon the x-ray structure, for the seven methyl

TABLE II
A COMPARISON OF THE OBSERVED AND CALCULATED CHEMICAL SHIFTS AND
DISTANCES FOR THE SEVEN METHYL GROUPS WITHIN ~10 Å OF THE EF SITE

Observed		Calculated		
δ_p*	r(Å)‡	δ_p*	Nucleus	r(Å)
17.69	6.2	18.075	Leu86δ1	6.1
14.17	7.9	11.297	Val99γ2	9.0
§	‖	9.807	Ile97γ2	6.0
−0.365	‖	6.270	Ile97δ1	7.2
−1.44	‖	6.120	Leu86δ2	8.4
−1.621	‖	−1.037	Ile58δ1	10.2
−1.90	‖	−3.793	Ile58γ2	9.6

*Ranked in order of decreasing shift in ppm.
‡Calculated from linewidths.
§Not shifted outside the diamagnetic spectrum.
‖The field dependence of the linewidths has not been determined.

groups within $\simeq 10$ Å of the EF binding site. One can see that there is fair agreement for the two most downfield shifted methyl groups (17.69 vs. 18.075) and 14.17 vs. 11.297). In addition, the predicted distances to the metal (6.1 and 9.0 Å) correspond well with the observed distances (6.2 and 7.9 Å) which were calculated from the linewidths of these resonances. However there is less agreement between the observed and calculated chemical shifts for the remaining five methyls.

A list of the most downfield and most upfield observed and calculated shifts is presented in Table III. The six most downfield observed shifts are in the range of 18.90–27.62 ppm. Three resonances with shifts >27.62 ppm are calculated. The six most upfield shifted resonances have observed chemical shifts of -12.68 to -19.06 ppm. Sixteen resonances with chemical shifts more upfield than -19.06 ppm are predicted. Also indicated in Table III is the predicted linewidth of the shifted resonances relative to the linewidth of the peak at 29.80 ppm. This calculation is based upon an r^6 dependence of the linewidth and a calculated distance from the observed linewidth of 5.9 Å for the peak at 19.80 ppm.

TABLE III

A COMPARISON OF THE MOST UPFIELD AND MOST DOWNFIELD OBSERVED AND
CALCULATED CHEMICAL SHIFTS

Observed	Calculated		
δ_P	δ_p	Nucleus	Relative Broadening*
	47.473	Asp90β	3.50
	35.455	Glu101β	2.71
	32.949	Asp94β	3.66
27.62	27.191	Gly95α	0.64
25.77	26.634	Asp90β	1.36
22.26	26.011	Gly93α	1.69
22.09	25.914	Asp94α	0.78
20.10	24.024	Ile97γ	3.64
18.90	17.618	Glu101γ	4.41
-12.86	-13.332	Phe57α	0.25
-14.16	-13.536	Lys96ϵ	0.10
-14.53	-13.628	Glu59γ	0.08
-14.60	-17.281	Lys96ϵ	0.12
-16.20	-17.921	Phe57β	0.14
-19.06	-20.128	Asp92β	3.81
	-28.628	Lys96δ	0.59
	-28.814	Ser91α	0.44
	-29.154	Ser91β	0.29
	-30.477	Lys96γ	0.59
	-31.068	Glu101γ	3.91
	-33.090	Phe57β	0.44
	-35.307	Asp92α	1.01
	-39.388	Lys96δ	0.68
	-40.338	Lys96γ	0.59
	-41.793	Lys96α	2.12
	-50.889	Asp92β	4.83
	-53.348	Phe57ϵ	14.11
	-57.797	Ser91β	1.25
	-95.357	Phe57δ	3.98
	-119.548	Lys96β	8.60
	-148.459	Lys96β	7.46

*This column indicates the predicted line broadening relative to the linewidth of the resonance with δ_{OBS} of 29.80 ppm and $r = 5.85$ Å (which was calculated from its linewidth); this predicted line broadening is based on a r^6 dependence (see Theory section).

DISCUSSION

The above strategy rests upon two major assumptions supported by other work: that it is the EF calcium which is replaced first, and that the lanthanides replace the calcium with no change in structure.

The x-ray crystallographic evidence indicates the protein contains two metal binding sites. The CD calcium is surrounded by six protein ligands and is not solvent accessible whereas the EF calcium includes one water molecule and five protein ligands in the primary coordination sphere. Two pieces of evidence indicate that lanthanides preferentially occupy this EF site. The isomorphous replacement of Ca^{+2} by Tb^{+3} in parvalbumin (10) at low Tb_o/P_o ratios results in the increase of electron density at the EF site. Only when the Tb_o/P_o ratios are significantly increased is there any additional Tb^{+3} occupancy in the CD site. Thus both sites can be filled, but the EF site is the site initially occupied. Laser induced luminescence experiments confirm in solution this order of occupancy (11). In these experiments a pulsed dye laser is used to excite the 4f electrons of europium or terbium bound to parvalbumin. OH oscillators in the first coordination sphere provide an efficient means of radiationless deexcitation of the Ln^{+3} ions, whereas OD oscillators are inefficient. Since the rate of deexcitation is directly proportional to the number of OH oscillators in the first coordination sphere, this number can be evaluated. For parvalbumin, the decay rates in both H_2O and D_2O solutions have been analyzed with the final conclusion that only one water molecule is coordinated to the metal. By analogy to the initial x-ray structure of the calcium parvalbumin complex (6), these solvent accessible Ln^{+3} ions are in the EF Ca^{++} site.

The isomorphous replacement of calcium ions in proteins by lanthanides provides a potential spectroscopic and magnetic resonance probe for the determination of the structure of calcium binding proteins. The validity of this substitution has been demonstrated in the case of trypsinogen activation (33). The lanthanide Nd^{+3} mimics Ca^{++} biologically, resulting in the acceleration of the activation of trypsinogen into trypsin. Structural x-ray crystallographic studies of lanthanides bound to thermolysin (34) also reveal that substitution results in little disruption of the structural integrity of the metal binding sites. Similarly the substitution of Ca^{+2} by Tb^{+3} in parvalbumin (10) results in little structural perturbation as determined by x-ray crystallography. The laser induced fluorescent decay constants of europium and terbium substituted parvalbumin (11) demonstrate there is one water molecule coordinated to the metal. The lanthanide substitution does not result in an increase of water coordination over that observed for the Ca^{++}-bound protein. This result that the Ln^{+3} ions in the EF site are six coordinate, taken together with the known preference of Ln^{+3} ions for higher coordination, implies that the protein and not the metal determines the structure of the protein metal complex. Thus there exist multiple lines of evidence to support that substitution of Ca^{+2} by Ln^{+3} is a nonperturbing probe of parvalbumin. To be fair, especially in terms of the conclusions to be drawn below, there is a question of the resolution of the x-ray results relative to small structural changes. When the diamagnetic Lu^{+3} is substituted for the EF Ca^{+2} in parvalbumin, a small number of minor changes in the ^1H-NMR spectrum of the protein can be ascertained. It is impossible, however, to determine the exact cause of the shifts.

The result of our NMR fitting procedure is that we are able to choose a set of parameters which give calculated NMR shifts which fit the observed shifts of the assigned His 26 C_2, His 26 C_4, and N-acetyl methyl resonances quite well. These resonances are far removed (13–20 Å) from the metal ion so that there is no possibility of a contact contribution to the shifts, and small errors in the x-ray structure such as the less well defined electron density in the region of the amino terminus are not going to greatly influence the calculated shifts. Also the

diamagnetic positions of these resonances are independently determined. Therefore we feel that our choice of best fit is not ambiguous, nor are any of the assumptions made likely to be incorrect for these resonances.

As we move in toward the metal ion, the agreement between the calculated and observed spectra gets worse. The situation is fair for the methyl groups which are 6–11 Å from the metal ion especially considering potential inaccuracies in the determination of the diamagnetic shifts and the use of the "centroid" model for the average methyl proton position. The calculated and observed distances agree quite well as an additional indication of the correctness of the best fit solution.

The agreement between calculated and observed shifts is very poor, however, for the nuclei close into the metal. Indeed we were not able to find any fit based upon reasonable criteria which did not give calculated shifts way outside the range of the observed shifts. While it is possible that some nearby nuclei are shifted outside of the observed range and also broadened beyond detection (see relative linewidth prediction in Table III), and it might be possible that some very nearby nuclei have compensating contact shifts, neither explanation could account for a large number of the nuclei which are calculated to have very large shifts. Another potential problem is internal motions in the protein. One would expect, however, the observed NMR shifts to be too large rather than too small reflecting an unequal weighting of closer conformations in averages of the sort of $<1/r^3>$. We feel that the biggest source of error is inaccuracies in the x-ray structure based proton coordinates at a level below the resolution of the x-ray method (1.9 Å in this case). That is, errors of the order of 0.5 Å in the position of nuclei as close as 3–4 Å, while not detectable in the x-ray method, greatly influence the NMR results. We hope to generate a refined structure with the aid of the NMR data at a level of resolution presently unobtainable by x-ray methods.

REFERENCES

1. Kretsinger, R. H. 1976. *Ann. Rev. of Biochemistry* **45**:239–266.
2. Rasmussen, H., D. B. P. Goodman, and A. Tenehouse. 1972. The role of cyclic AMP and calcium in cell activation. *C. R. C. Crit. Rev. Biochemistry* **1**:95–148.
3. Potter, J. D., J. D. Johnson, J. R. Dedman, W. E. Schreiber, F. Mandel, R. L. Jackson, and A. R. Means. 1977. Calcium binding proteins: relationship of binding structure, conformation and biological function. *In* Calcium Binding Proteins and Calcium Function. R. J. Wasserman, R. A. Corradino, E. Carafoli, R. H. Kretsinger, D. H. MacLennan, and F. L. Siegel, editors. Elsevier-North Holland, New York. 239–249.
4. Weeds, A., P. Wagner, R. Jakes, and J. Kendrick-Jones. 1977. Structure and function of myosin light chains. *In* Calcium Binding Proteins and Calcium Function. R. H. Wasserman, R. A. Corradino, E. Carafoli, R. H. Kretsinger, D. H. MacLennan and F. L. Siegel, editors. Elsevier-North Holland, New York. 222–231.
5. Stevens, F. C., M. Walsh, H. C. Ho, T. S. Teo and J. H. Wang. 1976. Comparison of calcium binding proteins. Bovine heart and brain protein activators of cyclic nucleotide phosphodiesterase and rabbit skeletal muscle troponin C. *J. Biol. Chem.* **251**:4495–4500.
6. Kretsinger, R. H. and C. E. Nockolds. 1973. Carp muscle calcium binding protein. *J. Biol. Chem.* **248**:3313–3326.
7. Weeds, A. G. and A. D. McLachlan. 1974. Structural homology of myosin alkali light chains, troponin C and carp calcium binding protein. *Nature (Lond.).* **252**:646–649.

8. Collins, J. H. 1974. Homology of myosin light chains, troponin C and parvalbumins deduced from comparison of their amino acid sequences. *Biochem. Biophys. Res. Commun.* **58**:301–308.

9. Collins, J. H. 1976. Homology of myosin DTNB light chain with alkali light chains, troponin C and parvalbumin. *Nature (Lond.).* **259**:699–700.

10. Sowadski, J., G. Cornick, and R. H. Kretsinger. 1978. Terbium replacement of calcium in parvalbumin. *J. Mol. Biol.* **124**:123–132.

11. Horrocks, W. DeW., Jr., and D. R. Sudnick. 1979. Lanthanide ion probes of structure in biology. Laser induced luminescence of decay constants provide a direct measure of the number of metal coordinated water molecules. *J. Am. Chem. Soc.* **101**:334–340.

12. Campbell, I. D., C. M. Dobson, and R. J. P. Williams. 1975. Nuclear magnetic resonance studies on the structure of lysozyme in solution. *Proc. R. Soc. Lond. A.* **345**:41–59.

13. Agresti, D. G., R. E. Lenkinski, and J. D. Glickson. 1977. Lanthanide induced perturbations of HEW lysozyme: evidence for non-axial symmetry. *Biochemistry Biophys. Res. Commun.* **76**:711–719.

14. Marinetti, T. D., G. H. Snyder, and B. D. Sykes. 1977. Nitrotyrosine chelation of nuclear magnetic resonance shift probes in proteins: application to bovine pancreatic trypsin inhibitor. *Biochemistry* **16**:647–653.

15. Marinetti, T. D., G. H. Snyder, and B. D. Sykes. 1975. Lanthanide interactions with nitrotyrosine. A specific binding site for nuclear magnetic resonance shift probes in proteins. *J. Am. Chem. Soc.* **97**:6562–6570.

16. Marinetti, T. D., G. H. Snyder, and B. D. Sykes. 1976. Nuclear magnetic resonance determination of intramolecular distances in bovine pancreatic trypsin inhibitor using nitrotyrosine chelation of lanthanides. *Biochemistry* **15**:4600–4608.

17. McDonald, C. C. and W. D. Phillips. 1969. Perturbation of the PMR spectrum of lysozyme by Co^{+2}. *Biochemistry Biophys. Res. Commun.* **35**:43–51.

18. Lenkinski, R. E., D. G. Agresti, D. M. Chen, and J. D. Glickson. 1978. An analysis of the Co^{+2} induced nuclear magnetic resonance perturbations of hen egg white lysozyme. *Biochemistry* **17**:1463–1468.

19. Carver, J. P., B. H. Barber, and B. J. Fuhr. 1977. Magnetic resonance studies of concanavalin A. Assignment of histidine resonances in 220 MHz proton spectrum of complexes with Co^{+2} and Zn^{+2}. *J. Biol. Chem.* **252**:3141–3146.

20 Bleaney, B. 1972. Nuclear magnetic resonance shifts in solution due to lanthanide ions. *J. Magn. Reson.* **8**:91–100.

21. Briggs, J. M., G. P. Moss, E. W. Randall, and K. D. Sales. 1972. Pseudo-contact contributions to lanthanide-induced nuclear magnetic resonance shifts. *J. Chem. Soc. Chem. Commun.* 1180–1182.

22. Reuben, J. 1973. On the origin of chemical shifts in lanthanide complexes and some implications thereof. *J. Magn. Reson.* **11**:103–104.

23. Vega, A. J. and D. Fiat. 1976. Nuclear relaxation processes of paramagnetic complexes. The slow motion case. *Mol. Phys.* **31**:347–355.

24. Gueron, M. 1975. Nuclear relaxation in macromolecules by paramagnetic ions: A novel mechanism. *J. Magn. Reson.* **19**:58–66.

25. Darnall, D. W. and R. G. Wilkins. 1980. High resolution NMR. *In* Methods for Determining Metal Ion Environments in Proteins. Advances in Inorganic Biochemistry. L. Lee and B. D. Sykes, editors. Elsevier-North Holland, New York, 183–210.

26. Shannon, R. D. 1976. Revised effective ionic radii and systematic studies of inter-atomic distances in halides and chalcogenides. *Acta Cryst.* **A32**:751–767.

27. Donato, Jr., H., and R. B. Martin. 1974. Conformation of carp muscle calcium binding protein. *Biochemistry* **13**:4575–4579.

28. McGarvey, B. R. 1979. Temperature dependence of the pseudocontact shift in lanthanide shift reagents. *J. Magn. Reson.* **33**:445–455.

29. Solomon, I. 1955. Relaxation processes in a system of two spins. *Phys. Rev.* **99**:559–565.

30. Nelson, D. J., S. J. Opella, and O. Jardetzky. 1976. ^{13}C nuclear magnetic resonance study of molecular motions and conformational transitions in muscle calcium binding parvalbumins. *Biochemistry* **15**:5552–5560.

31. Moews, P. C., and R. H. Kretsinger. 1975. Refinement of the structure of carp muscle calcium binding parvalbumin by model building and difference Fourier analysis. *J. Mol. Biol.* **91**:201–228.

32. Rowan, R., III, J. A. McGammon, and B. D. Sykes. 1974. A study of the distances obtained from nuclear Overhauser effect and relaxation time measurements in organic structure determination. Distances involving internally rotating methyl groups. Application to cis- and trans-crotonaldehyde. *J. Am. Chem. Soc.* **96**:4773–4780.

33. Darnall, D. W., and E. R. Birnbaum. 1970. Rare earth metal ions as probes of calcium ion binding sites in proteins. Neodymium (III) acceleration of the activation of trypsinogen. *J. Biol. Chem.* **245**:6484–6488.

34. Matthews, B. W., and L. H. Weaver. 1974. Binding lanthanide ions to thermolysin. *Biochemistry* **13**:1719–1725.